

Constraining the Synthesis of the Lightest p Nucleus ^{74}Se

A. Tsantiri^{1,2,3,*††}, A. Spyrou^{1,2,‡}, E. C. Good^{1,§}, K. Bosmopotinis^{1,2}, P. Giuliani¹, H. Arora^{1,4}, G. Balk^{1,5}, L. Balliet^{1,2}, H. C. Berg^{1,2}, J. M. Berkman^{1,6}, C. Dembski^{1,7}, P. DeYoung^{1,5}, Pavel A. Denissenkov,^{8,9,3,††,‡‡}, N. Dimitrakopoulos^{1,4}, A. Doetsch^{1,2}, T. Gaballah^{1,10}, R. Garg¹, A. Henriques,¹, R. Jain^{1,2,||}, S. N. Liddick,^{1,6}, S. Lyons,¹¹, R. S. Lubna¹, B. Monteagudo Godoy^{1,5}, F. Montes¹, S. Nash¹, G. U. Ogudoro^{1,5}, J. Owens-Fryar^{1,2}, A. Palmisano-Kyle^{1,12}, J. Pereira,¹, A. Psaltis^{1,13,14,3,††}, A. L. Richard^{1,15,1}, L. Roberti^{1,16,17,18,19,3,††}, E. K. Ronning, H. Schatz^{1,2}, A. Sebastian,^{1,2}, M. Smith^{1,2}, M. K. Smith,¹, C. S. Sumithrarachchi,¹, C. Tinson^{1,2}, P. Tsintari^{1,4,¶}, N. Tubaro^{1,2,**}, S. Uthayakumaar¹, A. C. C. Villari¹, E. Weissling^{1,5}, and R. G. T. Zegers^{1,2}

¹Facility for Rare Isotope Beams, Michigan State University, East Lansing, Michigan 48824, USA

²Department of Physics and Astronomy, Michigan State University, East Lansing, Michigan 48824, USA

³NuGrid Collaboration

⁴Department of Physics, Central Michigan University, Mount Pleasant, Michigan 48859, USA

⁵Physics Department, Hope College, Holland, Michigan 49423, USA

⁶Department of Chemistry, Michigan State University, East Lansing, Michigan 48824, USA

⁷Department of Physics, University of Notre Dame, Notre Dame, Indiana 46556, USA

⁸Department of Physics and Astronomy, University of Victoria, Victoria, British Columbia V8W 2Y2, Canada

⁹CaNPAN

¹⁰Department of Physics and Astronomy, Mississippi State University, Mississippi State, Mississippi 39762, USA

¹¹Pacific Northwest National Laboratory, Richland, Washington 99352, USA

¹²Department of Physics and Astronomy, University of Tennessee, Knoxville, Tennessee 37996, USA

¹³Department of Physics, Duke University, Durham, North Carolina 27710, USA

¹⁴Triangle Universities Nuclear Laboratory, Duke University, Durham, North Carolina 27710, USA

¹⁵Department of Physics and Astronomy, Ohio University, Athens, Ohio 45701, USA

¹⁶Istituto Nazionale di Fisica Nucleare—Laboratori Nazionali del Sud, Via Santa Sofia 62, Catania I-95123, Italy

¹⁷Konkoly Observatory, Research Centre for Astronomy and Earth Sciences,

Konkoly-Thege Miklós út 15-17, 1121 Budapest, Hungary

¹⁸CSFK HUN-REN, MTA Centre of Excellence,

Konkoly Thege Miklós út 15-17, Budapest H-1121, Hungary

¹⁹Istituto Nazionale di Astrofisica—Osservatorio Astronomico di Roma,

Via Frascati 33, Monte Porzio Catone I-00040, Italy



(Received 25 June 2025; revised 26 September 2025; accepted 29 October 2025; published 20 November 2025)

We provide the first experimental cross section of the $^{73}\text{As}(p,\gamma)^{74}\text{Se}$ reaction to constrain one of the main destruction mechanisms of the p nucleus ^{74}Se in explosive stellar environments. The measurement was done using a radioactive ^{73}As beam at effective center-of-mass energies of 2.9 and 2.3 MeV/nucleon. Along with the total cross-section measurement, statistical properties of the ^{74}Se compound nucleus were extracted, constraining the reaction cross section in the upper Gamow window of the γ process. The impact of the experimentally constrained reaction rate on ^{74}Se production in Type II supernovae was investigated through Monte Carlo one-zone network simulations. The results indicate that the overproduction of ^{74}Se by Type II supernova models cannot be resolved by nuclear physics alone and point toward the need for a more detailed understanding of the astrophysical conditions of relevance for the γ process.

DOI: 10.1103/d7dr-h36j

*Contact author: artemis.tsantiri@uregina.ca

†Present address: Department of Physics, University of Regina, Regina, Saskatchewan S4S 0A2, Canada.

‡Contact author: spyrou@frb.msu.edu

§Present address: Pacific Northwest National Laboratory, Richland, Washington 99352, USA.

||Present address: Lawrence Livermore National Laboratory, 7000 East Avenue, Livermore, California 94550-9234, USA.

¶Present address: Facility for Rare Isotope Beams, Michigan State University, East Lansing, Michigan 48824, USA.

**Present address: Department of Physics, University of Notre Dame, Notre Dame, Indiana 46556, USA.

††<http://nugridstars.org>

‡‡<https://canpan.ca>

Beyond iron, there is a group of rare, stable, neutron-deficient isotopes between ^{74}Se and ^{196}Hg known as the p nuclei. Even though they constitute only a small fraction of the heavy nuclear species, understanding their production mechanism has been a fundamental question in nuclear astrophysics since the field's inception [1] and remains a focus of research today [2–4]. The most widely accepted scenario for the formation of p nuclei is the γ process, which involves the disintegration of preexisting neutron-rich heavy seed material through a series of photon-induced reactions [5–7]. This process is thought to occur in the ONe layers of Type II core collapse supernovae (CCSN) [8,9] and in thermonuclear Type Ia supernovae [2,10,11]. In such environments, high temperatures of $T \sim 2\text{--}3.5$ GK guide the nuclear flux through consecutive (γ, n) reactions toward unstable, proton-rich species, followed by a combination of (γ, p) or (γ, α) reactions. After the explosion, the produced radioactive isotopes decay back to stability via β^+ /electron capture decays, reaching the elusive p nuclei. As p -nuclei abundances cannot be derived from stellar spectra, our knowledge of their isotopic distribution in the Solar System comes primarily from primitive meteorites, which preserve a near-solar composition for many heavy elements, serving as the main benchmark in testing γ -process models [6,7].

Modeling the γ process requires a complex network of thousands of nuclear reactions, most of which involve radioactive nuclei. Due to the scarcity of experimental cross sections, reaction rates are typically determined from Hauser-Feshbach statistical model calculations [12]. However, those predictions become increasingly uncertain for reactions involving nuclei further from stability [6,13]. While several indirect approaches can help constrain these rates, direct measurements remain the most reliable since they best resemble the stellar environment where the reactions occur. It is therefore essential to perform direct measurements to reduce these uncertainties and improve the accuracy of theoretical models. Despite extensive experimental efforts over the past decades to measure cross sections relevant to the γ process on stable nuclei [14–23], until today there has been only one measurement involving a radioactive beam within the Gamow window [24] ($\sim 1.3\text{--}4.0$ MeV in the center-of-mass system [25]) and two at energies higher than those relevant for the γ process [26,27]. The combination of small cross sections and low radioactive beam intensities makes such measurements particularly challenging, and therefore, they remain an active pursuit at many radioactive beam facilities. In this Letter, we present the first measurement of the $^{73}\text{As}(p, \gamma)^{74}\text{Se}$ cross section within the γ -process Gamow window using a radioactive ^{73}As beam and investigate its impact on the production of the lightest p nucleus, ^{74}Se .

While CCSN models [28–31] show variations in the production of the p nuclei, ^{74}Se is often found to be overproduced compared to solar abundances [32]. To explore whether this overproduction arises from reaction-rate

uncertainties, the production and destruction mechanisms of ^{74}Se have been a topic of study for more than a decade. Specifically, the $^{74}\text{Se}(p, \gamma)^{75}\text{Br}$ [33–36], $^{70}\text{Ge}(\alpha, \gamma)^{74}\text{Se}$ [37], and $^{74}\text{Se}(n, \gamma)^{75}\text{Se}$ [38] reactions have been measured directly. The last unmeasured reaction that significantly affects the final ^{74}Se abundance is the $^{74}\text{Se}(\gamma, p)^{73}\text{As}$, which has been identified as a key reaction to destroy ^{74}Se [39].

As matter in the stellar plasma is thermally excited, it is often advantageous to experimentally measure the radiative capture reactions of positive Q value, in this case the $^{73}\text{As}(p, \gamma)^{74}\text{Se}$ reaction, to reduce the stellar enhancement effect [40]. The rate of their photon-induced counterparts can then be inferred through the detailed balance theorem [25]. In CCSN models [28–30], ^{74}Se is found to be mostly produced near the upper end of the γ -process temperature range, around 3 GK. The corresponding Gamow window for the $^{73}\text{As}(p, \gamma)^{74}\text{Se}$ reaction is between 1.7 and 3.5 MeV [25].

In this energy region, the theoretically predicted cross-section uncertainty arises primarily from uncertainties in the statistical properties of the ^{74}Se compound nucleus, namely, the nuclear level density (NLD) and γ -strength function (γ SF). This uncertainty can be quantified with open source statistical modeling codes such as TALYS [41]. For this particular reaction, the uncertainty calculated using default NLD and γ SF model parameters available within TALYS varies by a factor of ≈ 6 . However, it has been seen that, particularly for unstable isotopes, this approach may underestimate the theoretical uncertainty [42,43]. In this Letter, we provide the first cross-section measurement of the $^{73}\text{As}(p, \gamma)^{74}\text{Se}$ reaction within the Gamow window, as well as constraints in the statistical properties of ^{74}Se , significantly reducing the uncertainty of the final production of ^{74}Se in CCSN.

The experiment took place at the Facility for Rare Isotope Beams, Michigan State University. A radioactive ^{73}As beam was produced from a source sample evaporated in the batch-mode ion source [44,45]. The beam was charge bred to the 23^+ charge state, accelerated to 3.1 and 3.7 MeV/nucleon in the ReA reaccelerator facility [46], and delivered onto a hydrogen gas-cell target in the experimental end station. The γ rays produced by the reaction were detected using the Summing NaI(Tl) (SuN) detector [47] and were analyzed using the γ -summing technique [48]. A detailed description of the experimental setup and analysis technique can be found in Refs. [49,50] from the proof-of-principle experiment, and the main components are briefly summarized here.

The target was a 4-cm-long gas cell made of plastic positioned at the center of the SuN detector. It had a 2- μm -thick molybdenum (Mo) entrance window, a 5- μm -thick exit window, and was filled with hydrogen gas at a pressure of ≈ 600 Torr. The interior and the front surfaces of the cell were lined with tantalum to minimize beam interaction with

the plastic and to reduce background. Surrounding the target was the barrel-shaped SuN detector [47]. SuN is divided into eight optically isolated segments and can provide three main types of spectra: total absorption spectra (TAS), sum of segments (SoS), and multiplicity. TAS corresponds to the full energy deposited in the detector, SoS corresponds to the sum of the energy spectra recorded by each segment, and multiplicity indicates how many segments recorded energy in each event [48].

Proton capture on the ^{73}As beam forms a ^{74}Se compound nucleus at an excited state $E_X = Q + E_{CM}$, where $Q = 8.549(4)$ MeV [51] and E_{CM} is the total kinetic energy in the center-of-mass system. Adding all γ rays originating from a single cascade forms the so-called “sum peak” in the TAS spectrum with energy equal to E_X . The integral of the sum peak corresponds to the number of reactions detected, which represents the ratio of the number of reactions taking place and the number of projectiles impinging on the target, namely, the experimental yield, Y [47].

The sum peak had background contributions from two main sources: cosmic-ray background and beam-induced background. For the former, the Scintillating Cosmic Ray Eliminating ENsemble (SuNSCREEN), an array of nine plastic scintillator bars arranged in a roof-like configuration above SuN, was utilized as a veto detector [52]. Events recorded by SuN in coincidence with SuNSCREEN were rejected, reducing our cosmic-ray background by approximately a factor of 3. Any remaining cosmic-ray background contributions were removed by utilizing the pulsed structure of the beam. The beam was delivered in 80- μs -long pulses every 200 ms, and data were recorded continuously with two time gates: one for the beam-on intervals and another for the background data between pulses, which were normalized to the length of the time gates and subtracted. The beam-induced background originated mainly from fusion evaporation reactions of the beam with the molybdenum entrance foil. To account for this background, data were collected both with the cell filled with hydrogen gas and with it empty. After the cosmic-ray background subtraction, the empty-cell data were normalized on the high energies of the spectra (between 13 and 18 MeV), where no contributions are expected from the reaction of interest, and then subtracted from the filled-cell data. Finally, Doppler corrections were applied on a segment-by-segment basis, as described in Refs. [49,50,53]. The final sum peak, along with the filled-cell and scaled empty-cell data for the beam energy of 3.7 MeV/nucleon, is shown in Fig. 1.

In addition to Doppler broadening, the sum peak broadens due to energy straggling of the beam as it passes through the cell’s entrance foil, resulting in the broadened structure shown in Fig. 1. This straggling introduces a distribution of excitation energies E_X , which must be considered when calculating the detection efficiency, ϵ . Furthermore, the SuN detector’s efficiency depends on the

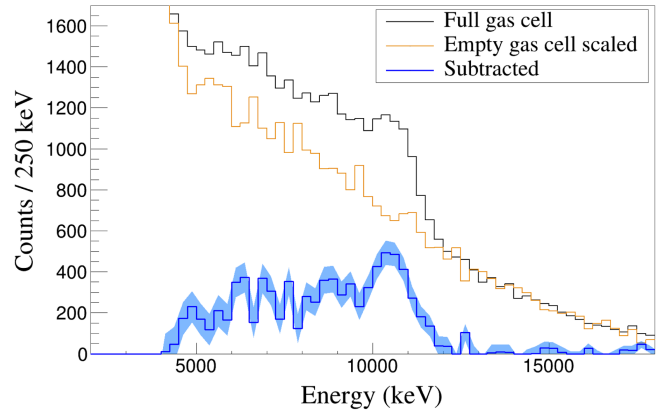


FIG. 1. Doppler-corrected TAS spectra showing the background subtraction for the sum peak for the $^{73}\text{As}(p, \gamma)^{74}\text{Se}$ reaction at beam energy of 3.7 MeV/nucleon. The black histogram corresponds to the gas cell filled with hydrogen gas, the orange histogram corresponds to the empty gas cell scaled, and the blue histogram is the fully subtracted sum peak with the band indicating the statistical uncertainty of the background subtraction.

multiplicity and energy of individual γ rays of each cascade [47]. To address these considerations in the efficiency calculation, the γ -ray deexcitation of each E_X contributing in the sum peak was simulated using the RAINIER code [54] and modeled to the detector’s response function using GEANT4 [55]. Further details on this process can be found in Refs. [49,50]. To avoid considering only s -wave proton capture, the spin and parity distribution of the simulated entry states in RAINIER was obtained from TALYS 1.96 [41]. The simulated TAS, SoS, and multiplicity spectra were fit using a χ^2 minimization code [56] to extract each E_X ’s contribution to the experimental spectra. The ratio of the experimental yield Y to the detector efficiency ϵ was calculated as a linear combination of integrals of the simulated sum peaks, weighted by each energy’s contribution.

The uncertainty associated with the ratio Y/ϵ was largely dominated by the statistical uncertainty of the background subtraction. For the measurement with beam energy of 3.7 MeV/nucleon, the statistical uncertainty was $\sim 18\%$. Unfortunately, the second measurement, with beam energy of 3.1 MeV/nucleon, suffered from very low statistics, and the associated uncertainty was $\sim 72\%$. Smaller contributions to the uncertainty included a $\sim 6\%$ uncertainty introduced from the normalization method of the empty-cell data as well as a $\sim 13\%$ uncertainty from the different statistical model inputs used in RAINIER. The overall uncertainties for Y/ϵ were $\sim 24\%$ and $\sim 74\%$ for the 3.7 and 3.1 MeV/nucleon beam energies, respectively. The efficiency in detecting γ rays from the deexcitation of the ^{74}Se compound nucleus was found to be 48(7)%. More details can be found in Ref. [57].

The target areal density was calculated from the average gas cell pressure recorded during each measurement and

TABLE I. Measured cross section of the $^{73}\text{As}(p,\gamma)^{74}\text{Se}$ reaction. The first column represents the initial beam energy in the laboratory system, and the second column the center-of-mass effective energy of the reaction. The third column shows the total number of incident particles, the fourth column the total number of reactions that occurred Y/ϵ , and the last shows the measured cross section.

Initial beam energy (MeV/nucleon)	Effective energy E_{eff} (MeV)	Total incident particles N_b	Total number of reactions Y/ϵ	Cross section σ (mb)
3.7	$2.95^{+0.05}_{-0.06}$	$(2.51 \pm 0.21) \times 10^{10}$	6193 ± 1480	3.11 ± 0.80
3.1	2.35 ± 0.05	$(1.67 \pm 0.14) \times 10^9$	152^{+112}_{-95}	$1.15^{+0.86}_{-0.73}$

the gas cell's dimension, with an associated uncertainty of $\sim 5\%$. The number of projectiles was calculated based on frequent current measurements on a Faraday cup directly upstream of the SuN detector, accounting for the beam charge state of 23^+ , which introduced an $\sim 8\%$ uncertainty to the total incident particles, N_b .

To account for the thickness of the hydrogen gas target, an effective center-of-mass energy, E_{eff} , was calculated as described in Ref. [58]. This energy corresponds to the point within the target where half of the reaction yield is produced. For nonresonant reactions, a linear decrease in cross section can be assumed across the volume of the target, where the beam loses approximately 250 keV, as calculated using SRIM [59]. The slope of the decreasing cross section along this energy range was obtained from statistical model calculations [60]. The thickness of the entrance Mo foil was measured using Rutherford back-scattering spectrometry at Hope College and was determined to be $1.93(12)$ mg/cm 2 , introducing an uncertainty of ~ 40 keV/nucleon in the beam energy. Additional uncertainty associated with E_{eff} includes the energy straggling of the beam as it traverses through the Mo foil ($\sim 2\%$) and the hydrogen gas ($\sim 1\%$) and the uncertainty of the beam energy delivered in ReA ($\sim 1\%$). The uneven energy

straggling distribution from SRIM led to asymmetric uncertainty in the effective energy.

The cross sections derived from experimental data (Table I) are shown in Fig. 2 compared with standard statistical model calculations using the NON-SMOKER [60] and TALYS 1.96 [41] codes. The color coding of the TALYS calculations is discussed in the next paragraphs. The calculated cross sections are in agreement within uncertainty of the NON-SMOKER cross section, but the central value is higher than the predictions by $\sim 18\%$ and $\sim 24\%$ for the higher and lower energies, respectively. The large statistical uncertainty of the lower energy data point vastly exceeds the spread of the TALYS predictions, and therefore, this data point is excluded for the remainder of this analysis. The higher-energy data point provides a strong constraint on the cross section and is used to constrain the statistical properties of the ^{74}Se compound nucleus.

The choice of the NLD and γ SF models in RAINIER significantly affects the shape of the simulated spectra, especially the SoS spectrum. Therefore, the ability of the NLD and γ SF model combinations to describe the simulated compound nucleus is reflected in the χ^2 from the fit of the TAS, SoS, and multiplicity spectra. In Ref. [49], this allowed for the identification of suitable parameter combinations for the analytical descriptions of the NLD and γ SF. In this Letter, this methodology was expanded to characterize all possible NLD and γ SF model combinations available in TALYS.

Within TALYS 1.96 there are six NLD [61–67], nine E1 [68–76], and three M1 [77] γ SF models available, as well as the ability to include a low-energy enhancement (upbend) in the M1 strength function [78–80]. The resulting 324 available NLD and γ SF model combinations were used as input in RAINIER, simulated in GEANT4, and fit to the experimental TAS, SoS, and multiplicity spectra as described above. The ability of each model combination to reproduce the experimental spectra was reflected in a “score” calculated based on the χ^2 of each model, as $\exp(-\chi^2/2N_{\text{bins}})$, where a higher score corresponds to a better description of the data. The normalization of the χ^2 to the number of data points (bins) in the respective spectrum, N_{bins} , was chosen such that each type of spectrum contributed equally to the overall score independently of how many bins it contained, an approach that has been adopted

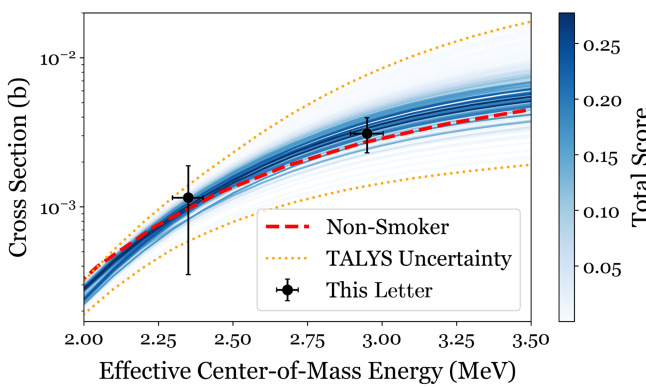


FIG. 2. The measured cross section of the $^{73}\text{As}(p,\gamma)^{74}\text{Se}$ reaction (black dots) compared with standard NON-SMOKER theoretical calculations [60], represented by a red dashed line, and default TALYS 1.96 calculations [41], depicted in blue lines. The color coding of the TALYS calculations reflects the ability of each model combination to simultaneously describe the experimental spectra and the calculated cross section. More details in text.

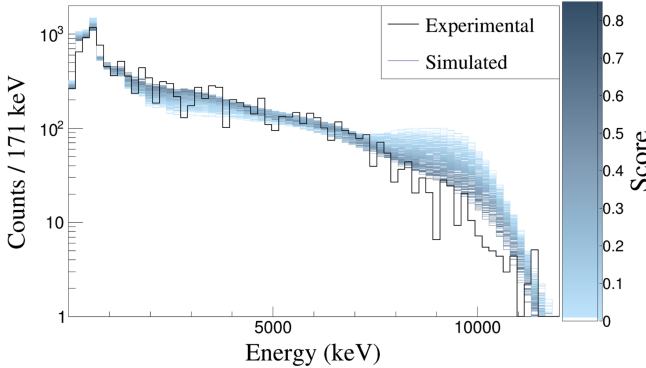


FIG. 3. The χ^2 minimization fits of the SoS spectrum for the $^{73}\text{As}(p, \gamma)^{74}\text{Se}$ reaction at a beam energy of 3.7 MeV/nucleon. The black line represents the experimental spectrum, and the various blue lines correspond to the simulated spectra for the combinations of the NLD and γ SF models from TALYS 1.96. The varying shades of blue in each line reflect different scores, where darker tones represent a better description of the experimental spectrum.

before in the calibration of nuclear models with contributions from multiple data types [81–83]. As an example, the comparison between the experimental and simulated spectra for the SoS is shown in Fig. 3. The simulated spectra, color coded based on their scores, correspond to default TALYS model combinations. Further investigation of the individual parameters of each model was beyond the scope of this Letter, as this methodology is sensitive only to the product of NLD and γ SF and not the individual absolute values.

Aside from their ability to reproduce the experimental spectra, the model combinations were also scored based on their proximity to the obtained cross section, accounting for the uncertainty in cross section and energy. The cross-section uncertainty was assumed to be Gaussian, whereas the energy uncertainty distribution was assumed to follow the energy straggling distribution from SRIM. More details on this calculation can be found in Ref. [57]. Two proton optical model potentials were considered, namely the default TALYS parametrization by Koning and Delaroche [84] as well as the description introduced by Jeukenne *et al.* [85,86] used by the NON-SMOKER code. The overall ability of each of the resulting 648 model combinations to simultaneously describe the experimental TAS, SoS, and multiplicity spectra along with the cross section was calculated from the product of all four scores and is reflected in the color of each TALYS calculation in Fig. 2.

To investigate the impact of this measurement on the production of ^{74}Se in CCSN, Monte Carlo one-zone simulations were performed using the NuGrid code PPN [87,88] in a similar manner as in Ref. [89]. The CCSN model was adapted from Ref. [30] for a $20M_{\odot}$ progenitor, although it should be noted that a similar impact is expected for any CCSN model reaching comparable peak

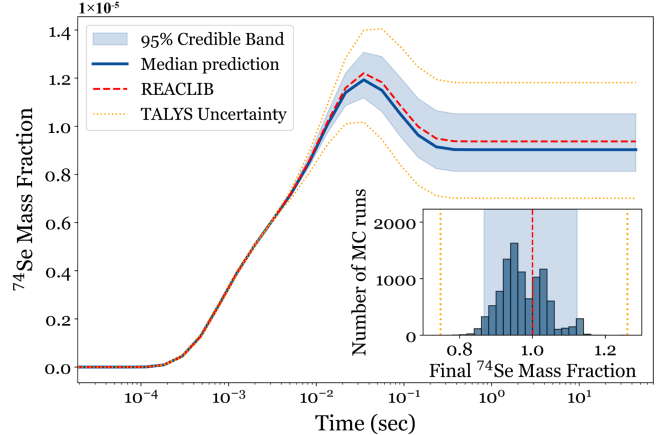


FIG. 4. Final ^{74}Se mass fraction produced during a $20M_{\odot}$ CCSN as a function of time calculated using NuGrid PPN one-zone simulations [87,88] (see text for details). The blue band corresponds to the 95th percentile of the MC sampled $^{73}\text{As}(p, \gamma)^{74}\text{Se}$ reaction rates with the median prediction shown in a darker blue line. The red dashed line corresponds to the default JINA-REACLIB reaction rate [93] and the orange dotted lines to the minimum and maximum reaction rates from TALYS 1.96. The inset shows the final ^{74}Se mass fraction distribution obtained in the MC simulations relative to JINA-REACLIB.

temperatures during the shock wave propagation. In the $20M_{\odot}$ model by Ref. [30], the maximum production of ^{74}Se occurs in the inner ONe layer, at mass coordinate $M = 2.93M_{\odot}$. Here, the temperature trajectory exhibited a plateau at peak temperature $T = 3.08$ GK.

The TALYS cross sections were converted to reaction rates, and for the peak temperature of $T = 3.08$ GK, each reaction rate was weighted based on the total score of the corresponding model, an approach akin to Bayesian model averaging [90–92]. From the resulting reaction rate distribution, 10 000 rates were randomly sampled in a Monte Carlo (MC) method, and in each realization of the PPN code, the rate of the $^{73}\text{As}(p, \gamma)^{74}\text{Se}$ reaction [and its inverse, $^{74}\text{Se}(\gamma, p)^{73}\text{As}$] was adjusted accordingly. The produced ^{74}Se mass fraction as a function of time is shown in Fig. 4. The blue band corresponds to the 95th percentile of the MC sampled rates with the median prediction shown in a darker blue line. The red dashed line corresponds to the mass fraction produced using the JINA-REACLIB rate [93] that adopts the NON-SMOKER cross section, and the orange dotted lines are the mass fractions obtained with the minimum and maximum rates obtained from TALYS 1.96.

As mentioned previously, the experimentally measured $^{73}\text{As}(p, \gamma)^{74}\text{Se}$ cross section used in the current simulations is $\sim 18\%$ higher than that of NON-SMOKER, which is adopted by the JINA-REACLIB database. That being said, the two rates are still consistent within experimental uncertainty, as shown in Fig. 2. Consequently, although a slightly lower mean ^{74}Se production is suggested here, the expected final ^{74}Se abundance from CCSN models

remains in good agreement with previous predictions using the JINA-REACLIB rate. Importantly, the presently reported abundance deviation is not enough to suggest that the observed overproduction of ^{74}Se in models of CCSN is driven by uncertainties in the $^{73}\text{As}(p,\gamma)^{74}\text{Se}$ reaction rate. Nevertheless, comparing the full width at half maximum of the distribution of final ^{74}Se mass fractions to the corresponding TALYS uncertainty shows that the measurement reduces the uncertainty due to this reaction rate by approximately a factor of 2, providing a more constrained and reliable input for future sensitivity studies. In conclusion, this Letter strongly constrains the most significant nuclear physics uncertainty related to the synthesis of ^{74}Se and indicates that the overproduction of ^{74}Se points toward the need for a more detailed understanding of the γ -process conditions such as a different seed distribution, density, temperature, or even a contribution from another process.

In summary, this Letter presents the first measurement of the $^{73}\text{As}(p,\gamma)^{74}\text{Se}$ reaction cross section using a radioactive ^{73}As beam and only the second radioactive beam experiment of a γ -process reaction within the Gamow window. The measured cross section was higher than the theoretical prediction from NON-SMOKER, but still in agreement within experimental uncertainty. The cross-section data, along with TAS, SoS, and multiplicity spectra, were used to characterize various nuclear level density and γ -ray strength function models from TALYS, allowing for the extraction of an experimentally constrained cross section across the entire Gamow window of the γ process. This characterization enabled the determination of an experimentally constrained reaction rate, which was used in Monte Carlo one-zone network simulations of the γ process in Type II supernovae. The uncertainty in the final ^{74}Se mass fraction from the $^{73}\text{As}(p,\gamma)^{74}\text{Se}$ reaction is reduced by a factor of two. This Letter resolves the remaining nuclear physics uncertainties affecting the production of ^{74}Se and indicates that changes in astrophysical models of the γ process are required to explain the solar p -nuclei abundances.

Acknowledgments—The authors would like to thank Aaron Chester and the Facility for Rare Isotope Beams (FRIB) Users Office for their support and assistance during the execution of the experiment and the ReA3 accelerator team for beam delivery. Additionally, we would like to thank the NuGrid Collaboration for providing the CCSN models and analysis codes and the International Research Network for Nuclear Astrophysics (IReNA) for enabling this collaboration through the IReNA Visiting Fellowship Program. The work was supported by the National Science Foundation under Grants No. PHY-1913554, No. PHY-2209429, and No. PHY-2209138 and by the U.S. National Nuclear Security Administration through Grant No. DE-NA0004071. This material is based upon work supported by the U.S. Department of Energy, Office of Science, Office of Nuclear Physics and used resources of FRIB,

which is a DOE Office of Science User Facility, operated by Michigan State University, under Award No. DE-SC0023633. This work was supported in part by the National Science Foundation under Grant No. OISE-1927130 (IReNA), the National Nuclear Security Administration under Award No. DE-NA0003180, and the Stewardship Science Academic Alliances program through DOE Award No. DOE-DE-NA0003906. P. D. acknowledges support from the Natural Sciences and Engineering Research Council of Canada (NSERC) Award No. SAPPJ-797 2021-00032 “Nuclear physics of the dynamic origin of the elements.” S. L. was supported by the Laboratory Directed Research and Development Program at Pacific Northwest National Laboratory operated by Battelle for the U.S. Department of Energy.

Data availability—The data that support the findings of this article are not publicly available. The data are available from the authors upon reasonable request.

- [1] E. M. Burbidge, G. R. Burbidge, W. A. Fowler, and F. Hoyle, Synthesis of the elements in stars, *Rev. Mod. Phys.* **29**, 547 (1957).
- [2] U. Battino, M. Pignatari, C. Travaglio, C. Lederer-Woods, P. Denissenkov, F. Herwig, F. Thielemann, and T. Rauscher, Heavy elements nucleosynthesis on accreting white dwarfs: Building seeds for the p-process, *Mon. Not. R. Astron. Soc.* **497**, 4981 (2020).
- [3] A. Choplin, S. Goriely, R. Hirschi, N. Tominaga, and G. Meynet, The p-process in exploding rotating massive stars, *Astron. Astrophys.* **661**, A86 (2022).
- [4] L. Roberti, M. Pignatari, A. Psaltis, A. Sieverding, P. Mohr, Zs.Fülpö, and M. Lugaro, The γ -process nucleosynthesis in core-collapse supernovae—I. A novel analysis of γ -process yields in massive stars, *Astron. Astrophys.* **677**, A22 (2023).
- [5] M. Arnould, Possibility of synthesis of proton-rich nuclei in highly evolved stars. II, *Astron. Astrophys.* **46**, 117 (1976), <https://ui.adsabs.harvard.edu/abs/1976A%26A...46..117A/abstract>.
- [6] T. Rauscher, N. Dauphas, I. Dillmann, C. Fröhlich, Z. Fülpö, and G. Gyürky, Constraining the astrophysical origin of the p-nuclei through nuclear physics and meteoritic data, *Rep. Prog. Phys.* **76**, 066201 (2013).
- [7] M. Pignatari, K. Göbel, R. Reifarth, and C. Travaglio, The production of proton-rich isotopes beyond iron: The γ -process in stars, *Int. J. Mod. Phys. E* **25**, 1630003 (2016).
- [8] S. E. Woosley and W. M. Howard, The p-processes in supernovae, *Astrophys. J. Suppl. Ser.* **36**, 285 (1978).
- [9] N. Prantzos, M. Hashimoto, M. Rayet, and M. Arnould, The p-process in SN 1987A, *Astron. Astrophys.* **238**, 455 (1990), <https://ui.adsabs.harvard.edu/abs/1990A%26A...238..455P/abstract>.
- [10] C. Travaglio, F. K. Röpke, R. Gallino, and W. Hillebrandt, Type Ia supernovae as sites of the p-process: Two-dimensional models coupled to nucleosynthesis, *Astrophys. J.* **739**, 93 (2011).

- [11] M. Kusakabe, N. Iwamoto, and K. Nomoto, Production of the p-process nuclei in the carbon-deflagration model for type Ia supernovae, *Astrophys. J.* **726**, 25 (2010).
- [12] W. Hauser and H. Feshbach, The inelastic scattering of neutrons, *Phys. Rev.* **87**, 366 (1952).
- [13] M. Arnould and S. Goriely, The p-process of stellar nucleosynthesis: Astrophysics and nuclear physics status, *Phys. Rep.* **384**, 1 (2003).
- [14] G. Gyürky, G. G. Kiss, Z. Elekes, Z. Fülöp, E. Somorjai, and T. Rauscher, Proton capture cross-section of $^{106,108}\text{Cd}$ for the astrophysical p-process, *J. Phys. G* **34**, 817 (2007).
- [15] G. Gyürky, M. Vakulenko, Z. Fülöp, Z. Halász, G. Kiss, E. Somorjai, and T. Szűcs, Cross section and reaction rate of $^{92}\text{Mo}(p,\gamma)^{93}\text{Tc}$ determined from thick target yield measurements, *Nucl. Phys. A* **922**, 112 (2014).
- [16] B. Mei, T. Aumann, S. Bishop, K. Blaum, K. Boretzky, F. Bosch, C. Brandau, H. Bräuning, T. Davinson, I. Dillmann *et al.*, First measurement of the $^{96}\text{Ru}(p,\gamma)^{97}\text{Rh}$ cross section for the p process with a storage ring, *Phys. Rev. C* **92**, 035803 (2015).
- [17] S. Harissopoulos, A. Spyrou, V. Foteinou, M. Axiotis, G. Provatas, and P. Demetriou, Systematic study of proton capture reactions in medium-mass nuclei relevant to the p process: The case of ^{103}Rh and $^{113,115}\text{In}$, *Phys. Rev. C* **93**, 025804 (2016).
- [18] A. Psaltis, A. Khaliel, E.-M. Assimakopoulou, A. Kanellakopoulos, V. Lagaki, M. Lykiardopoulou, E. Malami, P. Tsavalas, A. Zyriliou, and T. J. Mertzimekis, Cross-section measurements of radiative proton-capture reactions in ^{112}Cd at energies of astrophysical interest, *Phys. Rev. C* **99**, 065807 (2019).
- [19] A. Simon, R. Kelmar, O. Olivas-Gomez, E. Churchman, P. Milligan, C. S. Reingold, T. Anderson, A. M. Clark, N. Cooper, A. C. Dombos *et al.*, First measurements of capture reactions for the γ -process using HECTOR, *J. Phys. Conf. Ser.* **1308**, 012020 (2019).
- [20] A. Banu, E. G. Meekins, J. A. Silano, H. J. Karwowski, and S. Goriely, Photoneutron reaction cross section measurements on ^{94}Mo and ^{90}Zr relevant to the p -process nucleosynthesis, *Phys. Rev. C* **99**, 025802 (2019).
- [21] F. Heim, J. Mayer, M. Müller, P. Scholz, M. Weinert, and A. Zilges, Experimental techniques to study the γ process for nuclear astrophysics at the Cologne accelerator laboratory, *Nucl. Instrum. Methods Phys. Res., Sect. A* **966**, 163854 (2020).
- [22] H. Cheng, B.-H. Sun, L.-H. Zhu, M. Kusakabe, Y. Zheng, L.-C. He, T. Kajino, Z.-M. Niu, T.-X. Li, C.-B. Li *et al.*, Measurements of $^{160}\text{Dy}(p,\gamma)$ at energies relevant for the astrophysical γ process, *Astrophys. J.* **915**, 78 (2021).
- [23] P.-A. Söderström, A. Kuşoğlu, and D. Testov, Prospect for measurements of (γ, n) reaction cross-sections of p-nuclei at ELI-NP, *Front. Astron. Space Sci.* **10**, 1248834 (2023).
- [24] G. Lotay, S. A. Gillespie, M. Williams, T. Rauscher, M. Alcorta, A. M. Amthor, C. A. Andreou, D. Baal, G. C. Ball, S. S. Bhattacharjee *et al.*, First direct measurement of an astrophysical p -process reaction cross section using a radioactive ion beam, *Phys. Rev. Lett.* **127**, 112701 (2021).
- [25] C. Iliadis, *Nuclear Physics of Stars* (John Wiley & Sons, Ltd, New York, 2007).
- [26] J. Glorius, C. Langer, Z. Slavkovská, L. Bott, C. Brandau, B. Brückner, K. Blaum, X. Chen, S. Dababneh, T. Davinson *et al.*, Approaching the Gamow window with stored ions: Direct measurement of $^{124}\text{Xe}(p,\gamma)$ in the ESR storage ring, *Phys. Rev. Lett.* **122**, 092701 (2019).
- [27] S. F. Dellmann, J. Glorius, Y. A. Litvinov, R. Reifarth, L. Varga, M. Aliotta, F. Amjad, K. Blaum, L. Bott, C. Brandau *et al.*, First proton-induced cross sections on a stored rare ion beam: Measurement of $^{118}\text{Te}(p,\gamma)$ for explosive nucleosynthesis, *Phys. Rev. Lett.* **134**, 142701 (2025).
- [28] T. Rauscher, A. Heger, R. D. Hoffman, and S. E. Woosley, Nucleosynthesis in massive stars with improved nuclear and stellar physics, *Astrophys. J.* **576**, 323 (2002).
- [29] M. Pignatari, F. Herwig, R. Hirschi, M. Bennett, G. Rockefeller, C. Fryer, F. X. Timmes, C. Ritter, A. Heger, S. Jones, U. Battino, A. Dotter, R. Trappitsch, S. Diehl, U. Frischknecht, A. Hungerford, G. Magkotsios, C. Travaglio, and P. Young, NuGrid stellar data set. I. Stellar yields from H to Bi for stars with metallicities $Z = 0.02$ and $Z = 0.01$, *Astrophys. J. Suppl. Ser.* **225**, 24 (2016).
- [30] C. Ritter, F. Herwig, S. Jones, M. Pignatari, C. Fryer, and R. Hirschi, NuGrid stellar data set—II. Stellar yields from H to Bi for stellar models with $M_{\text{ZAMS}} = 1-25M_{\odot}$ and $Z = 0.0001-0.02$, *Mon. Not. R. Astron. Soc.* **480**, 538 (2018).
- [31] T. V. Lawson, M. Pignatari, R. J. Stancliffe, J. den Hartogh, S. Jones, C. L. Fryer, B. K. Gibson, and M. Lugaro, Radioactive nuclei in the early Solar system: Analysis of the 15 isotopes produced by core-collapse supernovae, *Mon. Not. R. Astron. Soc.* **511**, 886 (2021).
- [32] K. Lodders, Solar system abundances and condensation temperatures of the elements, *Astrophys. J.* **591**, 1220 (2003).
- [33] G. A. Krivonosov, O. L. Ekhichev, B. A. Nemashkalo, V. E. Storizhko, and V. K. Chirt, Radiative-capture cross sections of nuclides of intermediate atomic weight for low-energy protons, *Bull. Russ. Acad. Sci. Phys.* **41**, 175 (1977), <https://www-nds.iaea.org/exfor/servlet/X4sSearch5?chkAccnum=1&sort=entry&Accnum=A0048>.
- [34] G. Gyürky, Z. Fülöp, E. Somorjai, Z. Elekes, M. Kokkoris, S. Galanopoulos, P. Demetriou, S. Harissopoulos, S. Goriely, and T. Rauscher, $\text{Se}(p,\gamma)$ cross section measurements for p-process studies, *Nucl. Phys. A* **718**, 599 (2003).
- [35] Y. Skakun, S. Utentov, V. Mishchenko, J. Farkas, Z. Fülöp, G. Gyürky, G. G. Kiss, E. Somorjai, and T. Rauscher, Cross sections of low energy (p,γ) and (p,n) -reactions on selenium isotopes for the astrophysical γ -process, in *Proceedings of the 3rd International Conference on Current Problems in Nuclear Physics and Atomic Energy* (Kyiv, Ukraine, 2010), p. 207.
- [36] V. Foteinou, S. Harissopoulos, M. Axiotis, A. Lagoyannis, G. Provatas, A. Spyrou, G. Perdikakis, C. Zarkadas, and P. Demetriou, Cross section measurements of proton capture reactions on Se isotopes relevant to the astrophysical p process, *Phys. Rev. C* **97**, 035806 (2018).
- [37] Z. Fülöp, A. Kiss, E. Somorjai, C. Rolfs, H. Trautvetter, T. Rauscher, and H. Oberhummer, $^{70}\text{Ge}(\alpha,\gamma)^{74}\text{Se}$ cross section measurements at energies of astrophysical interest, *Z. Phys. A* **355**, 203 (1996).
- [38] I. Dillmann, M. Heil, F. Käppeler, T. Rauscher, and F.-K. Thielemann, Experimental (n, γ) cross sections of the p-process nuclei ^{74}Se and ^{84}Sr , *Phys. Rev. C* **73**, 015803 (2006).

- [39] W. Rapp, J. Goerres, M. Wiescher, H. Schatz, and F. Käppeler, Sensitivity of p-process nucleosynthesis to nuclear reaction rates in a $25M_{\odot}$ supernova model, *Astrophys. J.* **653**, 474 (2006).
- [40] T. Rauscher, G. G. Kiss, G. Gyürky, A. Simon, Z. Fülöp, and E. Somorjai, Suppression of the stellar enhancement factor and the reaction $^{85}\text{Rb}(p, n)^{85}\text{Sr}$, *Phys. Rev. C* **80**, 035801 (2009).
- [41] A. Koning, S. Hilaire, and S. Goriely, TALYS: Modeling of nuclear reactions, *Eur. Phys. J. A* **59**, 131 (2023).
- [42] D. Mücher *et al.*, Extracting model-independent nuclear level densities away from stability, *Phys. Rev. C* **107**, L011602 (2023).
- [43] A. Spyrou, D. Mücher, P. A. Denissenkov, F. Herwig, E. C. Good *et al.*, First study of the $^{139}\text{Ba}(n, \gamma)^{140}\text{Ba}$ reaction to constrain the conditions for the astrophysical *i* process, *Phys. Rev. Lett.* **132**, 202701 (2024).
- [44] A. C. Candia, G. Bollen, S. Campbell, A. Henriques, A. Lapierre, S. Nash, S. Schwarz, C. Sumithrarachchi, A. C. Villari, and K. A. Dommanich, Preparation of a 73As source sample for application in an offline ion source, *Appl. Radiat. Isot.* **217**, 111642 (2025).
- [45] C. Sumithrarachchi *et al.*, The new batch mode ion source for stand-alone operation at the Facility for Rare Isotope Beams (FRIB), *Nucl. Instrum. Methods Phys. Res., Sect. B* **541**, 301 (2023).
- [46] A. Lapierre, S. Schwarz, K. Kittimanapun, J. Rodriguez, C. Sumithrarachchi *et al.*, Commissioning results of the ReA EBIT charge breeder at the NSCL: First reacceleration of stable-isotope beams, *Nucl. Instrum. Methods Phys. Res., Sect. B* **317**, 399 (2013).
- [47] A. Simon, S. Quinn, A. Spyrou *et al.*, SuN: Summing NaI (Tl) gamma-ray detector for capture reaction measurements, *Nucl. Instrum. Methods Phys. Res., Sect. A* **703**, 16 (2013).
- [48] A. Spyrou, H.-W. Becker, A. Lagoyannis, S. Harissopoulos, and C. Rolfs, Cross-section measurements of capture reactions relevant to the p process using a 4π γ -summing method, *Phys. Rev. C* **76**, 015802 (2007).
- [49] A. Tsantiri, A. Palmisano-Kyle, A. Spyrou, P. Mohr, H. C. Berg, P. A. DeYoung, A. C. Dombos, P. Gastis, E. C. Good, C. M. Harris *et al.*, Cross-section measurement of the $^{82}\text{Kr}(p, \gamma)^{83}\text{Rb}$ reaction in inverse kinematics, *Phys. Rev. C* **107**, 035808 (2023).
- [50] A. Palmisano-Kyle, A. Spyrou, P. A. DeYoung, A. Dombos, P. Gastis, O. Olivas-Gomez, C. Harris, S. Liddick, S. M. Lyons, J. Pereira *et al.*, Constraining the astrophysical *p* process: Cross section measurement of the $^{84}\text{Kr}(p, \gamma)^{85}\text{Rb}$ reaction in inverse kinematics, *Phys. Rev. C* **105**, 065804 (2022).
- [51] W. Huang, M. Wang, F. Kondev, G. Audi, and S. Naimi, The AME 2020 atomic mass evaluation (I). Evaluation of input data, and adjustment procedures, *Chin. Phys. C* **45**, 030002 (2021).
- [52] E. Klopfer, J. Brett, P. A. DeYoung, A. C. Dombos, S. J. Quinn, A. Simon, and A. Spyrou, SuNSCREEN: A cosmic-ray veto detector for capture-reaction measurements, *Nucl. Instrum. Methods Phys. Res., Sect. A* **788**, 5 (2015).
- [53] S. Quinn, A. Spyrou, A. Simon *et al.*, First application of the gamma-summing technique in inverse kinematics, *Nucl. Instrum. Methods Phys. Res., Sect. A* **757**, 62 (2014).
- [54] L. Kirsch and L. Bernstein, RAINIER: A simulation tool for distributions of excited nuclear states and cascade fluctuations, *Nucl. Instrum. Methods Phys. Res., Sect. A* **892**, 30 (2018).
- [55] S. Agostinelli, J. Allison, K. Amako, J. Apostolakis, H. Araujo, P. Arce, M. Asai, D. Axen, S. Banerjee, G. Barrand *et al.*, GEANT4—A simulation toolkit, *Nucl. Instrum. Methods Phys. Res., Sect. A* **506**, 250 (2003).
- [56] A. C. Dombos, D.-L. Fang, A. Spyrou, S. J. Quinn, A. Simon, B. A. Brown, K. Cooper, A. E. Gehring, S. N. Liddick, D. J. Morrissey, F. Naqvi, C. S. Sumithrarachchi, and R. G. T. Zegers, Total absorption spectroscopy of the β decay of ^{76}Ga , *Phys. Rev. C* **93**, 064317 (2016).
- [57] A. Tsantiri, Proton-capture cross-section measurements for the astrophysical gamma process: From stable to radioactive ion beams, Ph.D. thesis, Michigan State University, 2025, <https://www.proquest.com/dissertations-theses/proton-capture-cross-section-measurements/docview/3219206471/se-2>.
- [58] C. Rolfs, W. Rodney, and W. Rodney, *Cauldrons in the Cosmos: Nuclear Astrophysics*, Theoretical Astrophysics (University of Chicago Press, Chicago, 1988).
- [59] J. F. Ziegler, M. Ziegler, and J. Biersack, SRIM—The stopping and range of ions in matter (2010), *Nucl. Instrum. Methods Phys. Res., Sect. B* **268**, 1818 (2010).
- [60] T. Rauscher and F.-K. Thielemann, Tables of nuclear cross sections and reaction rates: An addendum to the paper “Astrophysical Reaction Rates from Statistical Model Calculations,” *At. Data Nucl. Data Tables* **79**, 47 (2001).
- [61] T. Ericson, A statistical analysis of excited nuclear states, *Nucl. Phys.* **11**, 481 (1959).
- [62] A. Gilbert and A. G. W. Cameron, A composite nuclear-level density formula with shell corrections, *Can. J. Phys.* **43**, 1446 (1965).
- [63] A. V. Ignatyuk, K. K. Istekov, and G. N. Smirenkin, Collective effects in level density, and the probability of fission, *Sov. J. Nucl. Phys. (Engl. Transl.)* **30**, 5 (1979), <https://www.osti.gov/biblio/5176754>.
- [64] A. V. Ignatyuk, J. L. Weil, S. Raman, and S. Kahane, Density of discrete levels in ^{116}Sn , *Phys. Rev. C* **47**, 1504 (1993).
- [65] S. Goriely, F. Tondeur, and J. Pearson, A Hartree–Fock nuclear mass table, *At. Data Nucl. Data Tables* **77**, 311 (2001).
- [66] S. Goriely, S. Hilaire, and A. J. Koning, Improved microscopic nuclear level densities within the Hartree-Fock-Bogoliubov plus combinatorial method, *Phys. Rev. C* **78**, 064307 (2008).
- [67] S. Hilaire, M. Girod, S. Goriely, and A. J. Koning, Temperature-dependent combinatorial level densities with the D1M Gogny force, *Phys. Rev. C* **86**, 064317 (2012).
- [68] J. Kopecky and M. Uhl, Test of gamma-ray strength functions in nuclear reaction model calculations, *Phys. Rev. C* **41**, 1941 (1990).
- [69] D. Brink, Individual particle and collective aspects of the nuclear photoeffect, *Nucl. Phys.* **4**, 215 (1957).
- [70] P. Axel, Electric dipole ground-state transition width strength function and 7-MeV photon interactions, *Phys. Rev.* **126**, 671 (1962).

- [71] S. Goriely and E. Khan, Large-scale QRPA calculation of E1-strength and its impact on the neutron capture cross section, *Nucl. Phys.* **A706**, 217 (2002).
- [72] S. Goriely, E. Khan, and M. Samyn, Microscopic HFB + QRPA predictions of dipole strength for astrophysics applications, *Nucl. Phys.* **A739**, 331 (2004).
- [73] S. Goriely, Radiative neutron captures by neutron-rich nuclei and the r-process nucleosynthesis, *Phys. Lett. B* **436**, 10 (1998).
- [74] I. Daoutidis and S. Goriely, Large-scale continuum random-phase approximation predictions of dipole strength for astrophysical applications, *Phys. Rev. C* **86**, 034328 (2012).
- [75] S. Goriely, S. Hilaire, S. Péru, and K. Sieja, Gogny-HFB + QRPA dipole strength function and its application to radiative nucleon capture cross section, *Phys. Rev. C* **98**, 014327 (2018).
- [76] V. Plujko, O. Gorbachenko, R. Capote, and P. Dimitriou, Giant dipole resonance parameters of ground-state photo-absorption: Experimental values with uncertainties, *At. Data Nucl. Data Tables* **123–124**, 1 (2018).
- [77] R. Capote, M. Herman, P. Obložinský, P. Young, S. Goriely, T. Belgya, A. Ignatyuk, A. Koning, S. Hilaire, V. Plujko *et al.*, RIPL—Reference Input Parameter Library for calculation of nuclear reactions and nuclear data evaluations, *Nucl. Data Sheets* **110**, 3107 (2009).
- [78] A. Voinov, E. Algin, U. Agvaanluvsan, T. Belgya, R. Chankova, M. Guttormsen, G. E. Mitchell, J. Rekstad, A. Schiller, and S. Siem, Large enhancement of radiative strength for soft transitions in the quasicontinuum, *Phys. Rev. Lett.* **93**, 142504 (2004).
- [79] A. Simon, M. Guttormsen, A. C. Larsen, C. W. Beausang, P. Humby, J. T. Harke, R. J. Casperson, R. O. Hughes, T. J. Ross, J. M. Allmond *et al.*, First observation of low-energy γ -ray enhancement in the rare-earth region, *Phys. Rev. C* **93**, 034303 (2016).
- [80] A. C. Larsen, N. Blasi, A. Bracco, F. Camera, T. K. Eriksen, A. Görgen, M. Guttormsen, T. W. Hagen, S. Leoni, B. Million *et al.*, Evidence for the dipole nature of the low-energy γ enhancement in ^{56}Fe , *Phys. Rev. Lett.* **111**, 242504 (2013).
- [81] C. D. Pruitt, J. E. Escher, and R. Rahman, Uncertainty-quantified phenomenological optical potentials for single-nucleon scattering, *Phys. Rev. C* **107**, 014602 (2023).
- [82] A. E. Lovell, F. M. Nunes, J. Sarich, and S. M. Wild, Uncertainty quantification for optical model parameters, *Phys. Rev. C* **95**, 024611 (2017).
- [83] E. Alhassan, D. Rochman, A. Vasiliev, M. Hursin, A. J. Koning, and H. Ferroukhi, Iterative Bayesian Monte Carlo for nuclear data evaluation, *Nucl. Sci. Tech.* **33**, 50 (2022).
- [84] A. Koning and J. Delaroche, Local and global nucleon optical models from 1 keV to 200 MeV, *Nucl. Phys.* **A713**, 231 (2003).
- [85] J. P. Jeukenne, A. Lejeune, and C. Mahaux, Microscopic calculation of the symmetry and Coulomb components of the complex optical-model potential, *Phys. Rev. C* **15**, 10 (1977).
- [86] J.-P. Jeukenne, A. Lejeune, and C. Mahaux, Optical-model potential in finite nuclei from Reid's hard core interaction, *Phys. Rev. C* **16**, 80 (1977).
- [87] F. Herwig, S. Diehl, C. L. Fryer, R. Hirschi, A. Hungerford, G. Magkotsios, M. Pignatari, G. Rockefeller, F. X. Timmes, P. Young, and M. E. Bennet, Nucleosynthesis simulations for a wide range of nuclear production sites from NuGrid, in *Nuclei in the Cosmos (NIC X)* (2008), p. E23, [10.22323/1.053.0023](https://doi.org/10.22323/1.053.0023).
- [88] M. Pignatari and F. Herwig, The NuGrid research platform: A comprehensive simulation approach for nuclear astrophysics, *Nucl. Phys. News* **22**, 18 (2012).
- [89] P. A. Denissenkov, F. Herwig, G. Perdikakis, and H. Schatz, The impact of (n,γ) reaction rate uncertainties of unstable isotopes on the i-process nucleosynthesis of the elements from Ba to W, *Mon. Not. R. Astron. Soc.* **503**, 3913 (2021).
- [90] D. Phillips, R. Furnstahl, U. Heinz, T. Maiti, W. Nazarewicz, F. Nunes, M. Plumlee, M. Pratola, S. Pratt, F. Viens *et al.*, Get on the BAND wagon: A Bayesian framework for quantifying model uncertainties in nuclear dynamics, *J. Phys. G* **48**, 072001 (2021).
- [91] A. Hamaker, E. Leistenschneider, R. Jain, G. Bollen, S. Giuliani, K. Lund, W. Nazarewicz, L. Neufcourt, C. Nicoloff, D. Puentes *et al.*, Precision mass measurement of lightweight self-conjugate nucleus ^{80}Zr , *Nat. Phys.* **17**, 1408 (2021).
- [92] L. Neufcourt, Y. Cao, S. A. Giuliani, W. Nazarewicz, E. Olsen, and O. B. Tarasov, Quantified limits of the nuclear landscape, *Phys. Rev. C* **101**, 044307 (2020).
- [93] R. H. Cyburt, A. M. Amthor, R. Ferguson, Z. Meisel, K. Smith, S. Warren, A. Heger, R. D. Hoffman, T. Rauscher, A. Sakharuk, H. Schatz, F. K. Thielemann, and M. Wiescher, The JINA-REACLIB database: Its recent updates and impact on Type-I X-ray bursts, *Astrophys. J. Suppl. Ser.* **189**, 240 (2010).